

# The Effects of System Change on Buildings Equipped with Structural Systems with the Sandwich Composite Wall with J-Hook Connectors and Reinforced Concrete Shear Walls

Majid Saaly, Shahriar Tavousi Tafreshi, Mehdi Nazari Afshar

**Abstract**—The sandwich composite walls (SCSSC) have more ductility and energy dissipation than conventional reinforced concrete shear walls. SCSSCs have acceptable compressive, shear, in-plane bending, and out-of-plane bending capacities. The use of sandwich-composite walls with J-hook connectors has a significant effect on energy dissipation and reduction of dynamic responses of mid-rise and high-rise structural models. In this paper, incremental dynamic analyses for 10- and 15-story steel structures were performed under seven far-faults by OpenSees. The demand values of 10- and 15-story models are reduced by up to 32% and 45%, respectively, while the structural system change from shear walls (SW) to SCSSC.

**Keywords**—Sandwich composite wall, SCSSC, fling step, fragility curve, IDA, inter story drift ratio.

## I. INTRODUCTION

IN recent years, structural systems with the SCSSC have become very popular due to their ductility and ability to absorb and consume more energy than conventional reinforced concrete SWs. The application of this new system is in high-rise structures, nuclear power plant facilities, and bridge slabs are much more [1]. SCSSCs showed acceptable seismic performance under experimental tests and cyclic loading from the points of view of in-plane and out-of-plane shear and flexural interaction, in-plane punching shear, and compressive behavior [2]. Fig. 1 shows an example of a sandwich composite SW with a steel-concrete-steel cross-section [3], [4]. This paper compares the seismic behaviors of three-dimensional structures with cores consisting of SCSSCs with J-hook connectors and reinforced concrete SWs under far-fault records. The computational models of 10- and 15-story SCSSCs with J-hook connectors (SCWJ) and reinforced concrete SWs were developed using the OpenSees [5] finite element platform. These multi-layer SWs consist of square meshes of external steel plates and enclosed internal concrete cores, which are connected at their intersection with J-hooks (various elements including studs, etc.)

Majid Saaly and Mehdi Nazari Afshar are with the Azad University, West Tehran Branch, Tehran, Iran (e-mail: majid.saaly5@gmail.com, mehdi nazariafshar@gmail.com).

Shahriar Tavousi Tafreshi was with Azad University, West Tehran Branch, Department of Technical and Engineering Supervisor, Tehran, Iran, (e-mail: sh\_tavousi@iauctb.ac.ir).

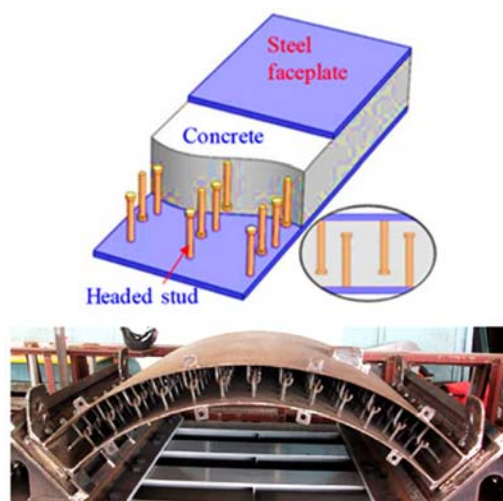


Fig. 1 The SCSSCs consisting of concrete and steel materials [1]

## II. REVIEW OF LITERATURE

SCWJs were originally developed for offshore structures and offshore installations. Their advantages include low economic costs, the possibility of using them at high deck heights, savings in execution and welding costs, and excellent seismic performance during earthquakes. The initial idea for SCSSJs was first proposed by Liew [2], [3] in 2008. In 2009, Liew and Sohel studied the static behavior of composite sandwich beams composed of J-hook connectors and lightweight concrete. In 2011, Sohel et al. studied the shear behavior of sandwich composites and shell planes connected by J-hooks used in Arctic installations [1]. In 2015, Liew and Yan [3] performed significant explosive tests on SCSSWJs, all of which confirmed the high strength and excellent performance of the SCSSJ under low-velocity projectile impacts and high-velocity blast loads. In 2009, Sohel et al. [2] studied the static behavior of sandwich beams made of ultra-lightweight cementitious composite materials, and in 2019, Yan et al. [1] continued these efforts. Most of these studies were based on determining the final strength of SCSSBJ structures [3]. In 2009, Sohel and Liew [1] examined the effects of projectiles on SCS protective sandwich walls, SCS sandwich beams and slabs with J-Hook joints. In addition, they developed numerical models to simulate the actual behavior of SCSSWJ under impact loads. The results showed

the superior behavior of SCSSBJ compared to the structures used previously. In 2016, Jan et al. [1] conducted large-scale experimental tests and numerical simulations on SCSSBJs to investigate the impact effects of ice fragments on composites. The results indicated that these structures have a very desirable and acceptable seismic performance [2]-[4].

### III. SIMULATION IN OPENSEES

In this paper, the seismic behavior of three-dimensional structures with cores consisting of SCSSCs equipped with J-hook connectors and reinforced concrete SWs under far-fault records were compared. The incremental dynamic analyses for three-spans 10- and 15-story steel structures were performed under seven far-faults. Fig. 2 shows the three-dimensional models studied in this research and Tables I and II show the specifications of beams, columns, and SWs of the models [6]-[8].

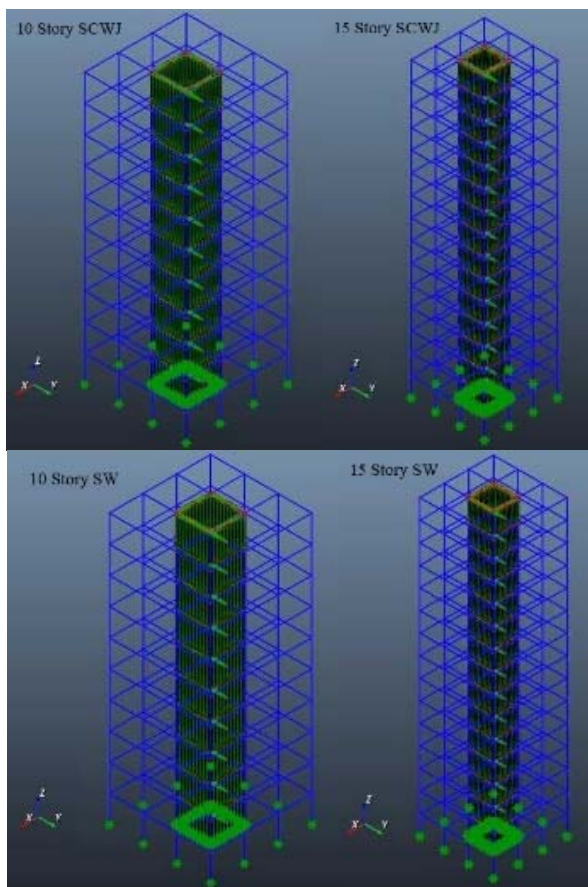


Fig. 2 10- and 15-story SCWJ, and SW buildings during running by OpenSees [5]

Incremental dynamic analyses were carried out for 10- and 15-story structures equipped with SCSSCs with J-hooks and reinforced SWs under seven far-fault records. Table III and Fig. 3 show the characteristics of far-fault earthquakes belonging to soil type III, and the response spectra of mentioned ones [6], [9].

TABLE I  
DETAILS OF SCWJ MODELS

| Level    | J-Hooks                     | SCWJ Depth (mm)        | Beams       | Columns       |
|----------|-----------------------------|------------------------|-------------|---------------|
| Roof     | HSS Section 100×100×8       | -                      | W550×250×12 | -             |
| 10 Story | 9 HSS Section 100×100×8     | 400                    | W550×250×12 | Box400×400×10 |
|          | 8 HSS Section 100×100×8     | 400                    | W550×250×12 | Box400×400×10 |
|          | 7 HSS Section 100×100×8     | 400                    | W550×250×12 | Box400×400×10 |
|          | 6 HSS Section 100×100×8     | 400                    | W550×250×12 | Box400×400×10 |
|          | 5 HSS Section 100×100×10    | 400                    | W550×300×12 | Box400×400×10 |
|          | 4 HSS Section 100×100×10    | 500                    | W550×300×12 | Box400×400×15 |
|          | 3 HSS Section 100×100×10    | 500                    | W550×300×12 | Box400×400×15 |
|          | 2 HSS Section 100×100×10    | 500                    | W550×300×12 | Box400×400×15 |
|          | 1 HSS Section 100×100×10    | 500                    | W550×300×12 | Box400×400×15 |
|          | Base                        | HSS Section 100×100×10 | 500         | -             |
| 15 Story | Roof HSS Section 100×100×10 | -                      | W550×250×12 | -             |
|          | 14 HSS Section 100×100×10   | 500                    | W550×250×12 | Box400×400×10 |
|          | 13 HSS Section 100×100×10   | 500                    | W550×250×12 | Box400×400×10 |
|          | 12 HSS Section 100×100×10   | 500                    | W550×250×12 | Box400×400×10 |
|          | 11 HSS Section 100×100×10   | 500                    | W550×250×12 | Box400×400×10 |
|          | 10 HSS Section 100×100×10   | 500                    | W550×250×12 | Box400×400×10 |
|          | 9 HSS Section 100×100×10    | 600                    | W550×250×12 | Box500×500×10 |
|          | 8 HSS Section 100×100×10    | 600                    | W550×250×12 | Box500×500×10 |
|          | 7 HSS Section 120×120×12    | 600                    | W550×250×12 | Box500×500×10 |
|          | 6 HSS Section 120×120×12    | 600                    | W550×300×12 | Box500×500×10 |
|          | 5 HSS Section 120×120×12    | 600                    | W550×300×12 | Box500×500×10 |
|          | 4 HSS Section 120×120×12    | 700                    | W550×300×12 | Box500×500×12 |
|          | 3 HSS Section 120×120×12    | 700                    | W550×300×12 | Box500×500×12 |
|          | 2 HSS Section 120×120×12    | 700                    | W550×300×12 | Box500×500×12 |
|          | 1 HSS Section 120×120×12    | 700                    | W550×300×12 | Box500×500×12 |
| Base     | HSS Section 120×120×12      | 700                    | -           | Box500×500×12 |

After performing the designs, to validate the OpenSees [5] algorithms, model of Yan et al. was used. Figs. 4 and 5 show the specifications and validity of the OpenSees algorithms [1], [3]. Table IV shows the period values of the 10- and 15-story models calculated by OpenSees software.

TABLE II  
DETAILS OF SW MODELS

| Level         | Rebar         | SCWJ Depth (mm) | Beams       | Columns     |            |
|---------------|---------------|-----------------|-------------|-------------|------------|
| Roof          | Φ 20 @ 400 mm | -               | W550×200×12 | -           |            |
| 10 Story      | Φ 20 @ 350 mm | 250             | W550×200×12 | Box         |            |
|               | Φ 20 @ 400 mm |                 |             | 350×350×10  |            |
|               | Φ 20 @ 350 mm | 250             | W550×200×12 | Box         |            |
|               | Φ 20 @ 400 mm |                 |             | 350×350×10  |            |
|               | Φ 20 @ 350 mm | 250             | W550×200×12 | Box         |            |
|               | Φ 20 @ 400 mm |                 |             | 350×350×10  |            |
|               | Φ 20 @ 300 mm | 250             | W550×200×12 | Box         |            |
|               | Φ 20 @ 350 mm |                 |             | 350×350×10  |            |
|               | Φ 22 @ 350 mm | 400             | W550×250×12 | Box         |            |
|               | Φ 20 @ 300 mm |                 |             | 400×400×12  |            |
|               | Φ 22 @ 350 mm | 400             | W550×250×12 | Box         |            |
|               | Φ 20 @ 300 mm |                 |             | 400×400×12  |            |
|               | Φ 22 @ 350 mm | 400             | W550×250×12 | Box         |            |
|               | Φ 20 @ 300 mm |                 |             | 400×400×12  |            |
|               | Φ 22 @ 350 mm | 400             | W550×250×12 | Box         |            |
|               | Φ 20 @ 300 mm |                 |             | 400×400×12  |            |
|               | Base          | Φ 22 @ 350 mm   | 400         | -           | 400×400×12 |
|               | Roof          | -               | -           | W550×250×12 | -          |
| 15 Story      | Φ 20 @ 300 mm | 400             | W550×250×12 | Box         |            |
|               | Φ 20 @ 200 mm |                 |             | 400×400×10  |            |
|               | Φ 20 @ 300 mm | 400             | W550×250×12 | Box         |            |
|               | Φ 20 @ 200 mm |                 |             | 400×400×10  |            |
|               | Φ 20 @ 300 mm | 400             | W550×250×12 | Box         |            |
|               | Φ 20 @ 200 mm |                 |             | 400×400×10  |            |
|               | Φ 22 @ 250 mm | 400             | W550×250×12 | Box         |            |
|               | Φ 22 @ 250 mm |                 |             | 400×400×10  |            |
|               | Φ 20 @ 250 mm | 400             | W550×250×12 | Box         |            |
|               | Φ 22 @ 250 mm |                 |             | 400×400×10  |            |
|               | Φ 20 @ 250 mm | 450             | W550×250×12 | Box         |            |
|               | Φ 22 @ 250 mm |                 |             | 500×500×10  |            |
|               | Φ 20 @ 250 mm | 450             | W550×250×12 | Box         |            |
|               | Φ 22 @ 250 mm |                 |             | 500×500×10  |            |
|               | Φ 20 @ 250 mm | 450             | W550×300×12 | Box         |            |
|               | Φ 22 @ 250 mm |                 |             | 500×500×10  |            |
|               | Φ 22 @ 250 mm | 450             | W550×300×12 | Box         |            |
|               | Φ 24 @ 250 mm |                 |             | 500×500×10  |            |
| Φ 22 @ 250 mm | 500           | W550×300×12     | Box         |             |            |
| Φ 24 @ 250 mm |               |                 | 500×500×12  |             |            |
| Φ 22 @ 250 mm | 500           | W550×300×12     | Box         |             |            |
| Φ 24 @ 250 mm |               |                 | 500×500×12  |             |            |
| Φ 22 @ 250 mm | 500           | W550×300×12     | Box         |             |            |
| Φ 24 @ 250 mm |               |                 | 500×500×12  |             |            |
| Base          | Φ 22 @ 250 mm | 500             | -           | Box         |            |
|               | Φ 24 @ 250 mm |                 |             | 500×500×12  |            |

The structures are assumed to be located in Tehran, an area with a very high relative risk (according to the earthquake zoning map of Iran 2800) [11]. The compressive strength of the steel was 290 MPa, and its elastic modulus was 199996 MPa. The strain hardening of the steel was 0.027. All structures were first designed in Sap2000 software and then modeled using OpenSees software.

TABLE III  
CHARACTERISTICS OF FAR-FAULT RECORDS [10]

| Name                 | Year | Station                                | Mw   | Distance (km) | PGA   |
|----------------------|------|--|------|---------------|-------|
| 1 Chuetsu-Oki        | 2007 | Kashiwazaki NPP_Unit 1: ground surface | 6.8  | 11.0          | 0.909 |
| 2 El Mayor-Cucapah   | 2010 | Riito                                  | 7.2  | 13.71         | 0.39  |
| 3 El Mayor-Cucapah   | 2010 | Cerro Prieto Geothermal                | 7.2  | 11.0          | 0.288 |
| 4 El Mayor-Cucapah   | 2010 | Michoacan De Ocampo                    | 7.2  | 16.0          | 0.538 |
| 5 Loma Prieta        | 1989 | Gilroy Array #4                        | 6.93 | 14.34         | 0.419 |
| 6 Morgan Hill        | 1984 | Gilroy Array #4                        | 6.19 | 11.54         | 0.349 |
| 7 Northwest China-03 | 1997 | Jiashi                                 | 6.1  | 17.73         | 0.3   |

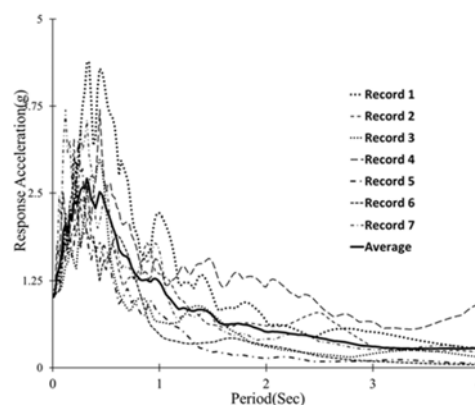
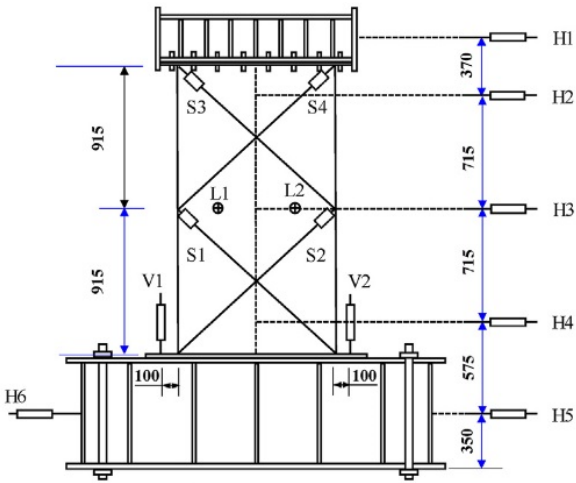
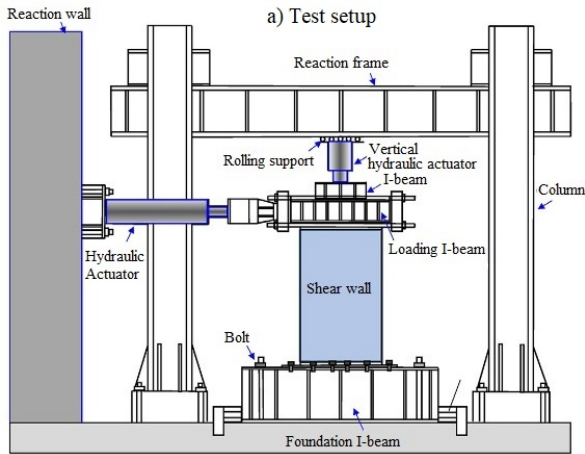
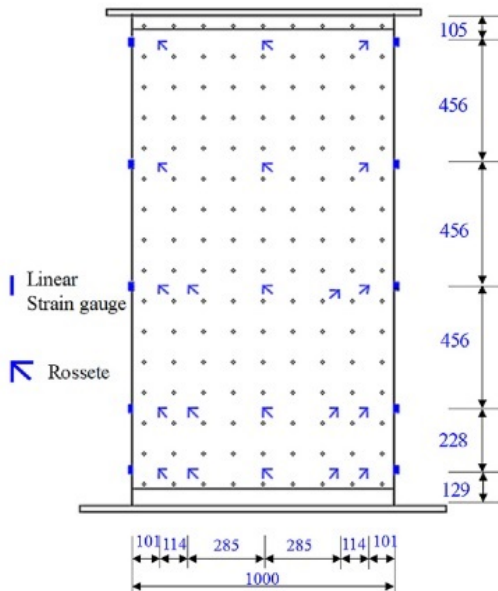


Fig. 3 Response spectra of the far earthquakes [10]

The Important factor I, response modification coefficient R, seismic zone coefficient A, and soil type are considered as 1, 7, 0.35, and III respectively. In all models, heights of the first floors are 4.0 meters and the other floors have 3.5 meters in height. The lengths of the bays are 6 meters. The rigid diaphragms were considered in all modeling of the floors. The foundation-to-column connections were assumed to be fixed. The dead load values of the floors and roof were 640 kg/m<sup>2</sup>, the live load of the floors was 200 kg/m<sup>2</sup>, and the live load of the roof was 150 kg/m<sup>2</sup> [11]-[14]. The SCSSCs and reinforced concrete SWs were defined by ShellMITC4 in OpenSees. The ShellMITC4 command simulates the real flexural behavior of thin plates using a combination of bilinear isoparametric formulation and modified shear interpolation [5]. The dimensions of the composite wall meshes are considered 50 cm by 50 cm, and J-hooks or composite wall connectors connect the two perimeter walls at the locations of these meshes. In all models, the beam-to-column connections were articulated rigid. The J-hooks were defined using nonlinear beam-column elements with the spread of plasticity along with elements. In the process of structural design, the requirements of FEMA P695 [14], Iranian National Building Codes [12], [13], and Standard no. 2800 [11] were considered. To evaluate more precisely, three-dimensional IDA analyses have been conducted under seven far-fault records using OpenSees [5]. All ground motions are of a magnitude of more than 6.5 and belong to soil type III according to Iranian Code No. 2800 (Fourth Edition) [11].



b) Layout of LVDTs (unit: mm)



c) Layout of strain gauges (unit: mm)

Fig. 4 Specifications of Yan model (a) Test setup, (b) Layout of VDTs, and (c) Layout of strain gauges. [1], [3]

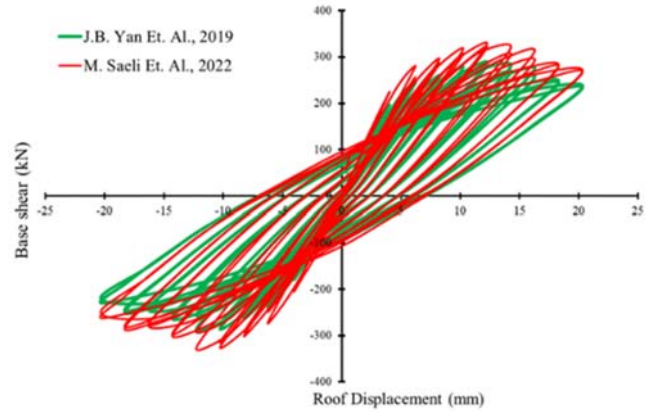


Fig. 5 Validity of Yan et al. model [1]

TABLE IV  
 PERIOD VALUES OF MODELS CALCULATED BY OPENSEES [5]

|                                 | Name | 10 story | 15 story |
|---------------------------------|------|----------|----------|
| Sandwich composite with J-hooks | T1   | 5.0      | 6.66     |
|                                 | T2   | 1.37     | 1.72     |
|                                 | T3   | 1.33     | 1.46     |
| Reinforced concrete SW          | T1   | 4.45     | 7.08     |
|                                 | T2   | 2.02     | 1.87     |
|                                 | T3   | 1.95     | 1.53     |

The damage measure (DM) and intensity measure (IM) were considered as the inter-story drift ratio and relatively efficient 5% damped first mode spectral acceleration,  $S_a(T1, 5\%)$ , respectively [6]. All steel materials are defined by the Steel02 command in OpenSees. All beams and columns are modeled by nonlinear beam-column elements with fiber sections. The masses of the floors were placed in the beam-column intersections as nodal masses. The horizontal record components with larger PGA values were used [14], [15].

#### IV. RESULTS OF IDA

Figs. 6 and 7 show IDA curves, and fractal curves of 10- and 15-story three- in three-span models with central cores surrounded by SCSSCs and reinforced SWs under far-fault records. As shown in the results, IDA curves cover a wide range of seismic demands (such as a spherical ball) under far-fault records. This point indicates that the selection of far earthquakes has been made intelligently. In all three-dimensional 10- and 15-story buildings, for all seismic intensities, the maximum inter-story drift values of SCWJ models are smaller than the SW models. When SCWJ is used, corresponding maximum inter-story drift values occur at higher seismic intensities than SW models. Therefore, the use of SCWJs has a significant effect on energy dissipation and reduction of dynamic responses of mid-rise and high-rise structural models. By changing the systems of the building from SW to SCWJ, the maximum inter-story drift values of 10- and 15-story models are reduced by up to 32% and 45%, respectively.

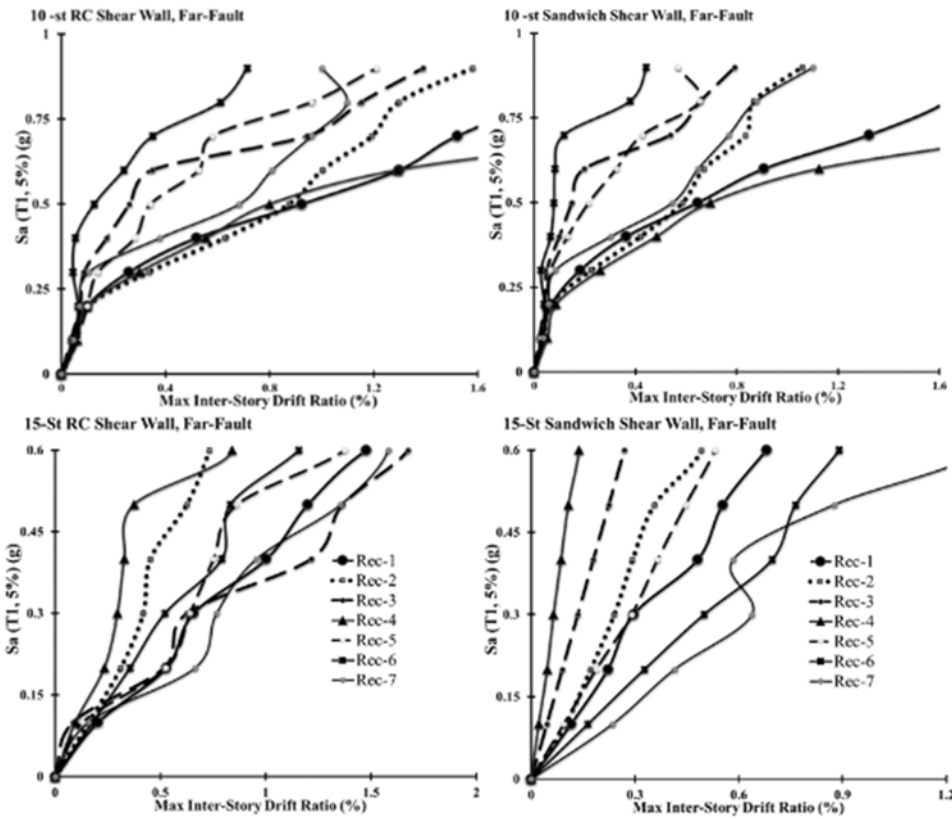


Fig. 6 IDA curves of 10- and 15-story models

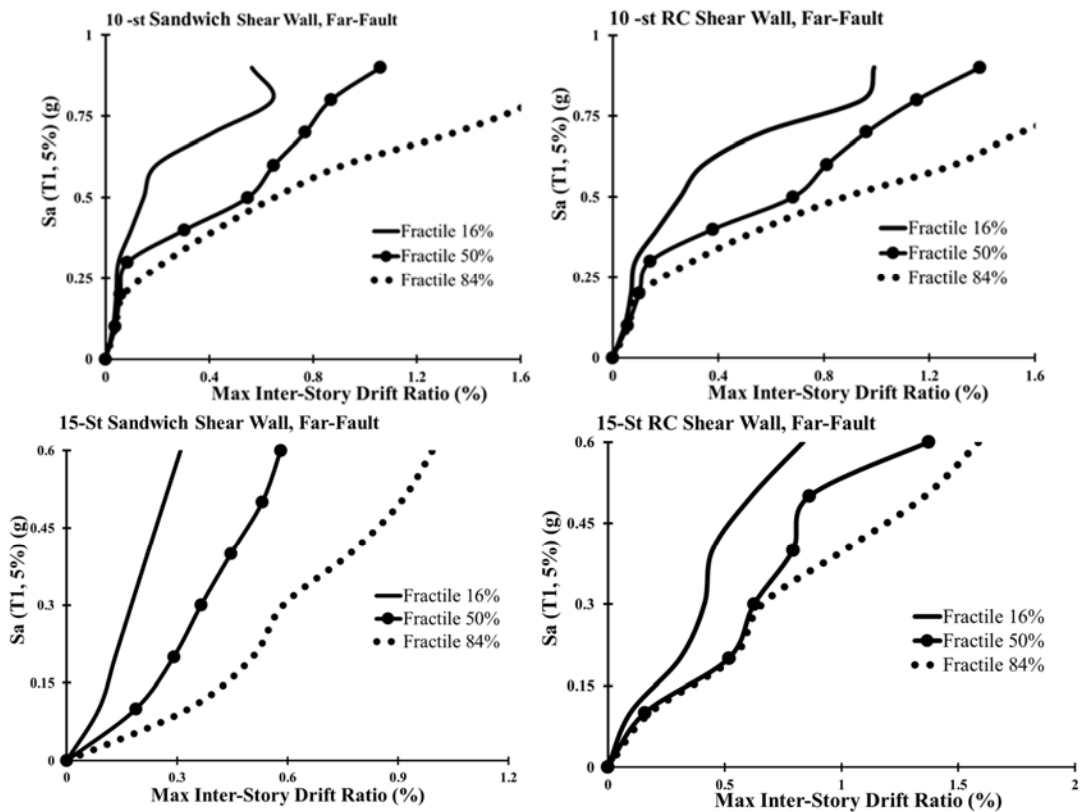


Fig. 7 Fractile curves of 10- and 15-story models

#### V.CONCLUSION

1. In all buildings, for all seismic intensities, the maximum inter-story drift values of SCWJ models are smaller than the SW models.
2. The use of SCWJs has a significant effect on energy dissipation and reduction of dynamic responses of mid-rise and high-rise structural models.
3. When SCWJ is used, corresponding maximum inter-story drift values occur at higher seismic intensities than SW models.
4. By changing the systems from SW to SCWJ, the demand values of 10- and 15-story models are reduced by up to 32% and 45%, respectively.

#### REFERENCES

- [1] Yan JB, Wang T., Li ZL., "Seismic behaviours of SCS sandwich shear walls using J-hook connectors," *Thin-Walled Structures*, 2019, 144: 106308.
- [2] Liew JYR, Soheli KMA., "Lightweight steel-concrete-steel sandwich system with J-hook connectors," *Eng. Struct.*, 2009, 31(5): 1166-1178.
- [3] Yan JB, Liew JYR., "Experimental and analytical study on ultimate strength behaviour of steel-concrete-steel sandwich composite beam structures," *Mater. Struct.*, 2015, 48(5): 1523-1544.
- [4] Wibowo A, Wilson JL, Lam N, Gad E. "Drift performance of lightly reinforced concrete columns. *Engineering Structures*," 2014;59:522-35.
- [5] OpenSees. "Open System for Earthquake Engineering Simulation. University of California," Berkeley, California: Pacific Earthquake Engineering Research Center; 2020.
- [6] Vamvatsikos D, Cornell CA. "Direct estimation of seismic demand and capacity of multidegree-of-freedom systems through incremental dynamic analysis of single degree of freedom approximation," *Journal of Structural Engineering*. 2005;131(4):589-99.
- [7] Bolt BA., "Seismic input motions for nonlinear structural analysis," *ISET journal of earthquake technology*, 2004, 41(2):223-32.
- [8] Chopra AK, Chintanapakdee C., "Comparing response of SDF systems to near-fault and far-fault earthquake motions in the context of spectral regions," *Earthquake engineering & structural dynamics*., 2001, 30(12):1769-89.
- [9] Kalkan E, Kunnath SK., "Effects of fling step and forward directivity on seismic response of buildings." *Earthquake spectra*. 2006;22(2):367-90.
- [10] Peer. Peer Ground Motion Database: Pacific Earthquake Engineering Research Center; 2015, Available from: <http://ngawest2.berkeley.edu/spectras/8475/searches/4547/edit>.
- [11] BHRC. Iranian Code of Practice for Seismic Resistant Design of Buildings: Standard no. 2800 (Fourth Revision) Iran Building and Housing Research Center; 2014.
- [12] MHUD. Iranian National Building Code for Structural Loadings (part 6), Third Revision, Tehran (Iran). Ministry of Housing and Urban Development. 2013.
- [13] MHUD. Iranian National Building Code (part 9): concrete structures design, Tehran (Iran). Ministry of Housing and Urban Development. 2009.
- [14] FEMA. Quantification of building seismic performance factors (FEMA P-695). Washington D.C.: Prepared by Applied Technology Council for the Federal Emergency Management Agency; 2009.
- [15] Hazus-MH MR-5, Multi Hazad loss Estimation Methodology: Earthquake Model. FEMA. Washington, D.C.: Department of Homeland security; 2003.